Thallium-201 SPECT Imaging of Brain Tumors: Methods and Results

Kenneth T. Kim, Keith L. Black, Donna Marciano, John C. Mazziotta, Barry H. Guze, Scott Grafton, Randall A. Hawkins, and Donald P. Becker

Department of Internal Medicine, Division of Neurosurgery, Division of Nuclear Medicine and Biophysics, Department of Radiological Sciences, UCLA School of Medicine, Los Angeles, California

Recent studies suggest that thallium-201 (^{201}Tl) planar scans of brain tumors more accurately reflect viable tumor burden than CT, MRI, or radionuclide studies with other single-photon emitting compounds. We have previously reported the utility of ^{201}Tl SPECT index in distinguishing low- from high-grade gliomas elsewhere. Here we describe the technical considerations of deriving a simple ^{201}Tl index, based on uptake in the tumor normalized to homologous contralateral tissue, from SPECT images of brain tumors. We evaluated the importance of consistently correcting for tissue attenuation, as it may achieve better lesion discrimination on qualitative inspection, and the methodologic limitations imposed by partial volume effects at the limits of resolution.

J Nucl Med 1990; 31:965–969

An ideal radiopharmaceutical for tumor localization should be readily available and have a high affinity for neoplastic tissue relative to normal tissue. A number of gamma emitting labeled tumor screening agents have previously been studied, including the radiolanthanides (*1*) gallium-67- (^{67}Ga) citrate, yttrerbium-169-citrate, fibrinogen-131, and mercury-197-chlormerodrin (*2*). All of these agents have significant drawbacks limiting their clinical utility.

We previously reported the value of an index of thallium uptake derived from single-photon emission computed tomography (SPECT) images of brain tumors in differentiating high-grade from low-grade lesions (*3*). In this work, we report the results of studies designed to optimize the data processing and generation of SPECT uptake indices.

Thallium-201, first used for myocardial imaging, was incidentally noted to show uptake in a lung carcinoma by Tonomi and Hisada (*4*). A subsequent study of untreated carcinoma, including lung, thyroid, liver, and esophageal cancer, demonstrated lesion visualization by ^{201}Tl uptake in 11 of 15 cases (*4*). Further observations suggested its utility in the diagnosis of cerebral lesions. There is substantial uptake in primary (*5*) and metastatic cerebral tumors (*6*) with little uptake in normal brain.

The potential clinical utility of ^{201}Tl reported in these early studies is probably related to its mechanism of localization. Actual uptake is related to a combination of factors including regional blood flow, blood brain barrier (BBB) permeability, and cellular uptake (*7*). Increased BBB permeability alone will not necessarily increase thallium uptake, since nonneoplastic lesions with increased BBB breakdown, such as areas of radiation necrosis or resolving hematomas, will have little or no ^{201}Tl uptake (*3*). Experimental evidence suggests that the ionic movement of thallium and potassium are related to active transport through an ATP cell membrane pump, and that ^{201}Tl uptake is related to cell growth rates (*8,9*).

Since thallium uptake does not simply rely on BBB breakdown, like iodinated contrast agents in computed tomography (CT) or gadolinium in magnetic resonance imaging (MRI), it is not surprising that Kaplan et al. (*10*) found ^{201}Tl to be superior to x-ray CT, ^{67}Ga, and technetium-99m-glucoheptonate in identifying variable, recurrent tumors in a series of 198 imaging studies done on 290 patients. Seven of Kaplan's patients had postmortem pathology which confirmed thallium uptake patterns. In a subsequent study of eight patients, Mountz et al. (*11*) reported the correlation of thallium uptake with tumor recurrence. These authors described a thallium index which was normalized to cardiac uptake and concluded that an increased ratio suggested tumor recurrence. However, these results were obtained from planar images of the head with standard gamma camera technology. SPECT provides improved lesion contrast, better three-dimensional localization of lesions, and cross-section images that facilitate comparison of the relative uptake in the tumor compared to homologous tissue. We analyzed several different meth-

Received May 8, 1989; revision accepted Dec. 26, 1989.

For reprints contact: Randall A. Hawkins, MD, PhD, Division of Nuclear Medicine and Biophysics, UCLA Center for the Health Sciences, Los Angeles, CA 90024-1721.

ods for determining a ^{201}Tl uptake index in an attempt to better define the technique and utility of this method of evaluating brain tumors.

MATERIALS AND METHODS

Patients

We performed 45 SPECT ^{201}Tl studies on 37 patients with primary brain tumors, 2 patients with metastatic lesions, 1 patient with a high-grade osteosarcoma, 1 patient with a hematoma, and 1 patient with toxoplasmosis. Of the 37 brain tumor patients, a group of 25 patients with both preoperative ^{201}Tl SPECT studies and available biopsy or autopsy information were analyzed to assess the correlation between thallium uptake and pathology. The brain histologic classification method of Kernohan (*12,13*) was used. This system includes four grades of primary astrocytoma (I, II, III, IV). The Grade IV lesion is commonly referred to as glioblastoma multiforme, while a Grade III is often known as an anaplastic astrocytoma, and the lower grade lesions (I and II) are generally referred to as "low-grade astrocytomas."

Thallium-201 Imaging

Each patient was injected with 4 mCi of ^{201}Tl in isotonic sodium chloride. SPECT images were initiated 5 min after injection, using the Siemens 7500 Digitrac Orbiter camera (Siemens Gammasonic, Des Plaines, IL). Images were acquired with 64 angular steps over 360° at 30 sec per view, with an average of 25,000 counts per view. We used a 20% symmetric window at 70 keV and a 15% window at 164 keV for photon detection. Each slice is one pixel thick or 6.47 mm. A 64×64 matrix with a Butterworth filter was used to reconstruct images in the transverse plane. Each study consisted of ~30–41 transverse slices which were group-added in pairs into half the number of slices. A uniformity correction matrix and a center of rotation correction was applied to each image. Each ^{201}Tl scan was processed for tissue attenuation using the method described by Chang (*14*) and available in the system software. The attenuation coefficient used was 0.12 cm^{-1}.

Defining Regions of Interest

Without knowledge of the histology of the lesion, operator-defined regions of interest (ROIs) were first drawn on the nonattenuation-corrected images in the slice showing the greatest activity in the tumor. Preoperative CT or MRI scans were used for anatomic guides. Using the system's ROI program, the homologous (contralateral) ROI could be easily determined by creating a mirror image of the initially defined region on the contralateral slide. Identical ROIs identified on the nonattenuation-corrected images could be superimposed on the identical transverse slice of interest of the group-added attenuation-corrected scan. For each patient, we thus determined the count densities, maximum counts/pixel as well as average counts/pixel, for the lesion and the homologous contralateral region on both the nonattenuation-corrected and attenuation-corrected scans.

When the tumor spanned several transverse slices, making it difficult to choose the most representative slice, we defined ROIs over several slices and used the mean value of the count densities in the regions. In two cases, the lesion was in the mid-line. In these cases, a mirror image ROI using a horizontal, rather than vertical axis of symmetry, was used. In another two cases, both high-grade lesions, there were two distinct lesions on both the thallium and the CT and/or MRI studies. It was assumed that the high-grade pathology applied to both lesions, and ^{201}Tl ratios were determined for each.

Statistical Analysis

Since we expected an increase in thallium uptake in tumors of higher grade, we compared the mean thallium index of low-grade versus high-grade lesions with a one-sided unpaired Student's t-test. Because attenuation correction might increase or decrease thallium uptake in tumors relative to the homologous area, we looked for a significant change in the ^{201}Tl index with a two-sided, paired Student's t-test.

RESULTS AND DISCUSSION

Choice of a Thallium Index

Mountz et al. (*11*) proposed a ^{201}Tl planar image uptake index of brain tumor counts normalized to cardiac blood-pool activity.

Although their calculated indices were clinically useful, there are two disadvantages to this approach. Timing of the cardiac acquisition will affect the relative distribution between blood-pool activity and myocardial uptake. Besides the added time needed to image a second organ system, more statistical variability was introduced because of the need to correct for differential counting times and background subtraction.

SPECT makes direct comparison with homologous tissue possible. Using the system's ROI program, one can define the homologous area to be exactly the same shape and size as the original ROI and place it in the contralateral hemisphere.

For each lesion, we routinely calculated three ratios:

Method 1: the maximum counts/pixel in the tumor over the maximum counts/pixel in the homologous ROI.

Method 2: the maximum counts/pixel in the tumor over the average counts/pixel in the homologous region.

Method 3: the average counts/pixel in the tumor over the average counts/pixel in the homologous region.

Table 1 illustrates the mean ^{201}Tl indices for each of these three methods, for both nonattenuation-corrected and attenuation-corrected scans.

Since the most aggressive part of a tumor might be represented by the area with the maximum counts, we decided to normalize the maximum counts in the tumor to the maximum counts in the homologous region in Method 1. The pixel in the tumor with the highest counts, however, is not necessarily normalized to the corresponding contralateral pixel but rather to the pixel with the highest counts in the homologous region. A ratio based on a single pixel from each region is subject to more statistical error. Indeed, this method did degrade the statistical comparison between low- and high-

TABLE 1
Mean Thallium Index

	Low-grade lesions (n = 14 lesions, 14 patients)	High-grade lesions (n = 13 lesions, 11 patients)
Method 1:		
Nonattenuation-corrected	1.24 ± 0.35	1.90 ± 0.54*
Attenuation-corrected	1.29 ± 0.36	2.03 ± 0.71†
Method 2:		
Nonattenuation-corrected	1.95 ± 0.64	3.34 ± 0.82*
Attenuation-corrected	1.99 ± 0.55	3.49 ± 1.05*
Method 3:		
Nonattenuation-corrected	1.21 ± 0.34	2.28 ± 0.49*
Attenuation-corrected	1.27 ± 0.40	2.40 ± 0.61*

* $p \leq 0.0005$, one-sided unpaired Student's t-test.
† $0.0005 < p \leq 0.005$, one-sided unpaired Student's t-test.
The values illustrated are the mean thallium index ± 1 s.d.

grade lesions; line 2 of Table 1 indicates a $p < 0.005$ rather than $p < 0.0005$.

The major methodologic problem with Method 1 is that the denominator, maximum counts in the homologous region, may often not reflect true homologous tissue, but other areas of high activity. We therefore calculated a ^{201}Tl uptake ratio based on maximum counts in the tumor normalized to average counts in the homologous region in Method 2. As expected, the numeric values of the indices are higher than in Method 1, and the method produced a greater statistical difference between ^{201}Tl uptake in low- and high-grade lesions (lines 3 and 4, Table 1).

Method 3 (ratio of average counts in tumor to average counts in homologous tissue) indices also confirm our primary finding of a strong statistical difference between low- and high-grade lesions (Table 1, lines 5 and 6). Using average counts achieved the same results as focusing on maximum counts probably because of the partial volume averaging across the tumors in the ROIs, although in some cases (see Figure 3) resolution was sufficient to delineate some internal structure of the lesions. On the other hand, with positron emission tomography (PET) studies of gliomas with fluorine-18-fluorodeoxyglucose (FDG), DiChiro reported the utility of maximum glucose metabolic rates rather than average glucose metabolic rates in identifying the most aggressive part of the tumor (*15*). This finding may reflect in part the higher resolution of most PET systems compared to gamma camera based SPECT systems as employed in this study.

Method 3 is the most reproducible method for calculating a ^{201}Tl index. It is less affected by tissue heterogeneity and ROI definition than Methods 1 and 2.

Effect of Attenuation Correction

To assess the effects of attenuation correction on the ^{201}Tl index, we first compared the thallium index in the nonattenuation-corrected versus the attenuation-corrected scans and found no statistical difference. One might expect that deeper lesions rather than peripheral lesions would be enhanced after attenuation correction. Therefore, we also looked at mid-line lesions separately. In this subgroup, attenuation correction had no significant influence in high-grade lesions ($p > 0.35$) where high thallium uptake is evident with or without attenuation correction. For nine low-grade mid-line lesions using average number of counts per pixel, there is a suggestion that attenuation correction alters the calculated ^{201}Tl index ($p = 0.09$). Indeed, attenuation correction results in better lesion discrimination on gross visual inspection in a few cases (Fig. 1). On the other hand, attenuation correction has little effect on the ^{201}Tl indices of peripheral lesions, both low- and high-grade. Our finding of a noticeable effect of attenuation correction only on low-grade, mid-line lesions is consistent with our a priori expectation that low-grade as opposed to high-grade and mid-line lesions as opposed to peripheral lesions would be most enhanced after attenuation correction.

Effect of Partial Volume

With any tomographic imaging system, as the object of interest decreases below twice the full width at half maximum (FWHM) of the in plane resolution, the apparent concentration of activity within any object will decrease (*16*). The image FWHM of our SPECT camera is ~9 mm (*17*) (8.7 mm without scatter to 9.6 mm with scatter) and, thus, average count densities in lesions <18 mm may be underestimated.

The size of the lesions can influence the count densities especially at the limits of resolution, where larger lesions may have increased average and maximum counts per pixel. We therefore evaluated the average area of the lesions in the two comparison groups, low- and high-grade, both on CT or MRI as well as on the thallium SPECT images. The average areas on CT or MRI images for low-grade lesions was 2.44 cm^2 ± 1.67

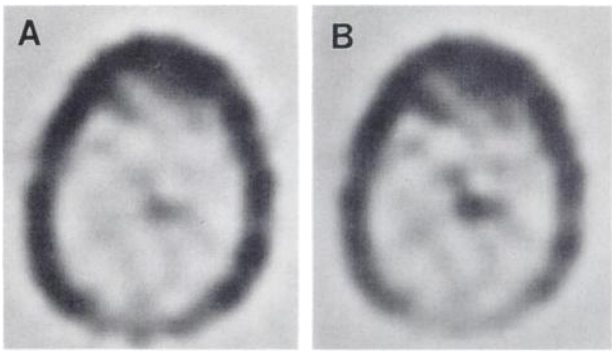

FIGURE 1
Effect of attenuation correction. (A) The SPECT ^{201}Tl image of a primary lymphoma without attenuation correction. (B) The SPECT ^{201}Tl image of the same lesion with attenuation correction.

cm^2 (±1 s.d.) and for high-grade lesions, 2.83 cm^2 ± 1.05 cm^2 ($p > 0.30$). Likewise, the mean number of pixels in a lesion on a thallium SPECT scan was 33.9 ± 16.7 (± 1 s.d.) for low-grade lesions and 41.9 ± 22.4 for high-grade lesions ($p > 0.30$). The mean lesion size was not significantly different on either CT/MRI or thallium SPECT studies, and therefore, lesion size per se cannot account for our findings of increased activity in high-grade lesions. Additionally, no correlation between uptake index and lesion size (determined by number of pixels in the ROI) was evident in the high-grade or low-grade groups.

Although the partial volume effect is minimized in large lesions, this problem can still result in a lower apparent uptake of thallium when metabolically inactive areas such as necrotic cores or tumor edema, are included in the area of interest. This effect is illustrated in two patients with high-grade lesions (Fig. 2). As expected from their pathology, both thallium scans show high uptake, but the resolution is insufficient to delineate a rim of tissue uptake, and, thus, ROIs around the entire hot spot are delineated in each case. Because Patient A's lesion had a large necrotic center, the calculated ^{201}Tl index is unusually low for a Grade IV lesion (1.81). Conversely, there is a less pronounced partial volume effect in Patient B, whose lesion consists of a smaller metabolically inactive center, and the ^{201}Tl index of this Grade III lesion remains high (3.07).

Another potential source of partial volume-related error in measured count densities in ROIs is contamination from adjacent high intensity structures, such as the scalp or facial structures. This effect is minimized with correctly placed ROIs.

Clinical Correlation

We found a strong statistical difference between the ^{201}Tl uptake indexes in low-grade versus high-grade lesions, as previously reported by Kaplan et al. (*10*), Mountz et al. (*11*), and Black et al. (*3*). In 14 patients with biopsy- or autopsy-documented low-grade astrocytomas, the mean ^{201}Tl index is 1.27 ± 0.40, as compared to a mean index of 2.40 ± 0.61 for all 11 patients with high-grade astrocytomas ($p < 0.0005$). Using a threshold index of 1.5 to distinguish low- versus high-grade lesions, we could predict the grade with an accuracy of 89%.

The only incorrectly predicted lesions using a ^{201}Tl index cut-off of 1.5 were three low-grade lesions with high indices. Two patients died within 6 mo of diagnosis, raising the question of whether ^{201}Tl uptake may correlate better with prognosis than the more commonly accepted standard of using histologic grade. In one patient with a ^{201}Tl index of 2.14, histologic diagnosis was obtained from stereotactic biopsy where sampling error may account for a misleading tumor grade.

Some calculated index values using our technique may be artificially decreased because of the partial volume effect, as illustrated in Figure 2. Of the four pathologically documented high-grade lesions whose indices are relatively low, between 1.5 and 2.0, three lesions had either probable edema or necrosis on x-ray CT within the lesion. The fourth patient had a second lesion with a ^{201}Tl index > 3.0, thus clearly identifying the patient as having a high-grade lesion.

In one case, the anatomic resolution of the SPECT thallium scan was sufficient to identify two areas of differential uptake that correlated with findings of mixed pathology (Fig. 3). There was an area of high uptake at the left frontal pole, ^{201}Tl index of 3.27, and a second area of moderate uptake posterior to the first, with a ^{201}Tl index of 1.38. The operative pathology showed an anaplastic astrocytoma in the frontal pole, but a more benign low-grade oligodendroma in the posterior region.

CONCLUSION

Thallium-201 is a useful radiopharmaceutical for preoperative evaluation of brain tumors. Since our ^{201}Tl uptake index correctly identified all high-grade lesions and suggested increased biologic malignancy in pathologic low-grade tumors with high indices, it may add

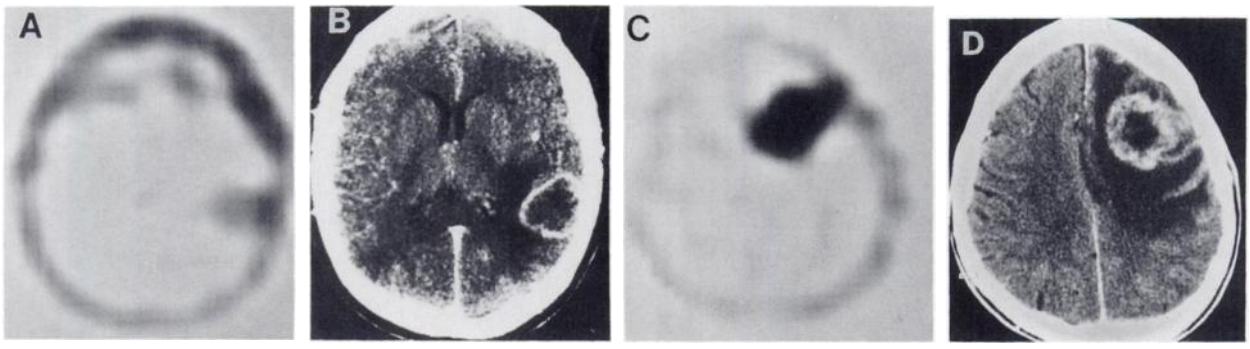

FIGURE 2
Patient A, with a Grade IV astrocytoma, has a thallium index of 1.81. (A) SPECT ^{201}Tl image and (B) x-ray CT image. Patient B, with a Grade III astrocytoma, has a thallium index of 3.07. (C) SPECT ^{201}Tl image and (D) x-ray CT. Note the more pronounced partial volume effect in Patient A, whose lesion contains a larger necrotic core.

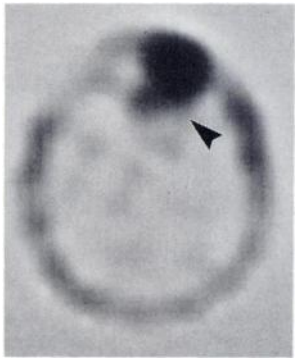

FIGURE 3
Anatomic resolution of ^{201}Tl SPECT. SPECT ^{201}Tl image demonstrating an area of high uptake at the left frontal pole, with a ^{201}Tl index of 3.27 and a second area of moderate uptake caudal to the first (arrow). Pathologic examination of the surgical specimen revealed an anaplastic astrocytoma in the frontal pole, but a more benign low-grade oligodendroma in the rest of the tumor.

useful clinical information on the biology of primary brain tumors. Our work is consistent with the findings of other investigators who noted thallium uptake in brain tumors with planar imaging. We developed a method that has been easily integrated into the routine processing of ^{201}Tl SPECT scans in our clinical nuclear medicine department. Thallium uptake indices using a ratio of average counts (Method 3) of suspected brain lesions are being routinely reported to the neurosurgeons. We recommend the routine use of attenuation correction. As expected, this correction has the most effect on low-grade lesions in the deep parenchyma and can result in better lesion discrimination on qualitative inspection. Although partial volume effects can cause an underestimation in the uptake index in a few selected cases, the resolution of SPECT is sufficient for utilizing this quantitative method clinically as reported recently (*3*).

REFERENCES

1. Hisada K, Ando A. Radiolanthanides as promising tumor scanning agents. *J Nucl Med* 1973; 14:615.
2. Hisada K. Tumor scanning and imaging. In: Sodee DB, Early PJ, eds. *Technology and interpretation of nuclear medicine procedures.* St. Louis: CV Mosby; 1972:416–428.
3. Black KL, Hawkins RA, Kim KT, et al. Thallium-201 (SPECT): a quantitative technique to distinguish low grade from malignant brain tumors. *J Neurosurg* 1989; 71:342–346.
4. Tonami N, Hisada K. Clinical experience of tumor imaging with 201-Tl-chloride. *Clin Nucl Med* 1977; 2:75–81.
5. Ancri D, Bassett JY, Lonchampt MF, Etarard C. Diagnosis of cerebral lesions by thallium-201. *Nucl Med* 1978; 128:417–422.
6. Ancri D, Bassett JY. Diagnosis of cerebral metastases by thallium-201. *Br J Radiol* 1980; 53:443–445.
7. Atkins HL, Budinger TF, Labowitz E, et al. Thallium-201 for medical use. Part 3: human distribution and physical imaging properties. *J Nucl Med* 1977; 18:133–140.
8. Elligsen JD, Thompson JE, Frey HE, et al. Correlation of (Na^+-K^+)ATPase activity with growth of normal and transformed cells. *Exp Cell Res* 1974; 87:233–240.
9. Dasarov LB, Friedman H. Enhanced Na^+-K^+ activated adenosise triphosphatase activity in transformed fibroblasts. *Cancer Res* 1974; 34:1862–65.
10. Kaplan WD, Takronan T, Morris H, et al. Thallium-201 brain tumor imaging: a comparative study with pathologic correlation. *J Nucl Med* 1987; 28:47–52.
11. Mountz JM, Stafford-Schuck K, McKeever PE, et al. Thallium-201 tumor/cardiac ratio estimation of residual astrocytoma. *J Neurosurg* 1988; 68:705–709.
12. Burger PC, Vogel FS. *Surgical pathology of the nervous system and its coverings.* New York: John Wiley and Sons; 1976:189–346.
13. Kernohan JW, Mabon RF, Svien HJ, Adson AW. A simplified classification of the gliomas. *Proc Staff Meet Mayo Clinic* 1949; 24:71–75.
14. Chang LT. A method for attenuation correction in a radionuclide computed tomography. *Trans Nucl Sci* 1978; NS-25:638–643.
15. DiChiro G, DeLaPaz RL, Brooks RA, et al. Glucose utilization of cerebral gliomas measured by [^{18}F]fluoro-deoxyglucose and positron emission tomography. *Neurology* 1982; 32: 1323–1329.
16. Sorenson JA, Phelps ME. *Physics in nuclear medicine,* 2nd edition. 1987:406–408.
17. Siemens Gammasonics, Inc. NEMA specifications. Publication #710-002150 Revision B (May 1984).

Editorial: Systematic Evaluation of Primary Brain Tumors

In the United States, 8,000 patients die each year of primary intracranial malignant tumors. Glioblastoma multiforme, the most common primary malignant brain tumors, accounts for 75% of gliomas in adults. For afflicted patients, the prognosis remains grim. Following operation and irradiation, the median survival is less than one year. Fewer than 10% of patients survive two years.

Neurooncologists are confronted with difficult diagnostic and therapeutic issues when providing care for patients suspected of harboring a primary brain tumor. Of major concern is the need to correctly diagnose a tumor of glial origin and to determine the grade of the tumor. The WHO grading classification separates glial tumors into three grades reflecting increasing degrees of malignant potential: Grade 1 (low-grade with median

Received Mar. 2, 1990; revision accepted Mar. 2, 1990.
For reprints contact: Michael L. Gruber, MD, Massachusetts General Hospital, Fruit St., Boston, MA.